https://doi.org/10.1016/j.yofte.2017.02.009

Signal Power Distribution Based Modulation Format Identification for Coherent Optical Receivers

Jie Liu[1,2], Kangping Zhong[2], Zhenhua Dong[3], Changjian Guo[4], Alan Pak Tao Lau[3], Chao Lu[2] and Yanzhao Lu[5]

[1]School of Electronics and Information Technology, Sun Yat-Sen University, Guangzhou 510006, China

[2] Photonics Research Centre, Department of Electronic and Information Engineering, The Hong Kong Polytechnic University, Hung Hom, Kowloon, Hong Kong

[3]Photonics Research Centre, Department of Electrical Engineering, The Hong Kong Polytechnic University, Hung Hom, Kowloon, Hong Kong

[4]South China Academy of Advanced Optoelectronics, South China Normal University, Guangzhou 510006, China

[5]Network Research Department, Huawei Technologies, Shenzhen, China

Corresponding author: Jie Liu (e-mail: liujie47@mail.sysu.edu.cn).

Abstract: A simple modulation format identification (MFI) technique based on extracting features from the statistical distributions of normalized signal power is proposed for cognitive coherent optical receivers. The proposed MFI technique requires no prior training and is independent of phase noise or frequency offset. Furthermore, it also performs good identification of the polarization-multiplexed (PM) M-QAM signals even after insufficient equalization of the constant modulus algorithm (CMA). Simulation results demonstrate successful MFI among PM-QPSK, PM-8-QAM, PM-16-QAM, PM-32-QAM and PM-64-QAM signals within OSNR range of practical system. Experimental verification using PM-QPSK/ 16-QAM/64-QAM signals generated from a pulse pattern generator (PPG) also confirms the feasibility of the proposed MFI technique after long distance fiber transmission.

Index Terms: modulation format identification, coherent optical receiver, digital signal processing

1. Introduction

The utilization of coherent detection and digital signal processing (DSP) has dramatically increased the capacity and transmission distance of optical fiber communications in the past few years [1]-[4]. However, only increasing the transmission capacity is not enough for the future bandwidth-desired optical network, because the current dense wavelength division multiplexing (DWDM) network with fixed wavelength grid cannot be fully utilized due to lack of spectrum flexibility. To properly address these challenges, cognitive optical networks (CON) [5] with flexible

transceivers and network elements have recently attracted a lot of interest. In the CON, reconfigurable transmitters are capable of signal generation with arbitrary modulation formats to adapt to real-time network conditions and data rate for a given traffic demand [6]. Therefore, prior knowledge of the modulation formats of the incoming signals at a receiver unit will no longer be guaranteed. As a result, it may become necessary for a digital coherent receiver to identify the modulation format of incoming signals at the physical layer before appropriate modulation-format -dependent signal processing is employed.

Modulation Format Identification (MFI) has been studied to a certain extent for wireless communication systems and has become an important component for software-defined radio (SDR) and military applications [7]. However, most proposed MFI methods in wireless networks are not tolerant to oscillator phase noise as electronic oscillators have significantly better frequency and phase accuracy than local lasers used in coherent optical communications [8]-[10]. In addition, the majority of frequency offset estimation (FOE) and carrier phase estimation (CPE) techniques in digital coherent receivers are somewhat dependent on modulation format in the first place [11]-[12], rendering the knowledge of modulation format a must. As a result, it is desirable to derive an MFI technique independent of phase noise for future CONs. Several MFI techniques for optical communication systems were recently proposed in the literature [13]-[17]. In [13], a MFI scheme based on signal constellation and K-means algorithm has been proposed. However, this scheme has limited tolerance to the phase noise and thus requires modulation-format-transparent algorithms before MFI. MFI technique utilizing artificial neural networks has been presented in [14], which can achieve high identification accuracy in the presence of fiber dispersion. However, prior training is needed for this technique. In [15]-[17], MFI methods based on stokes space signal representation for digital coherent optical receiver have been demonstrated, which allow for MFI at a considerably earlier stage of the DSP module in the receiver and therefore relax the subsequent modulation-format-dependent algorithms. Also, those schemes do not need training or a constellation diagram to operate. However, iterated machine learning algorithms are required in these methods, which may increase the computation complexity.

Recently, we proposed a simple MFI technique described in [18] that studies the distribution of received normalized signal power after CD compensation, timing phase recovery and constant modulus algorithm (CMA) equalization, as shown in Fig. 1. The MFI technique requires simple computations, needs no prior training and is independent of phase noise. However, the CMA cannot give effective equalization for the multi-level polarization multiplexed (PM) M-QAM signals [19], which will have an impact on the correct identification of modulation format. Actually, no comments about these problems were talked about in [18].

As a result, in this paper, we expand on our previous work in [18] and mainly focus on the MFI of PM-M-QAM signals after CMA pre-convergence. It is found that the correct MFI can be realized among PM-QPSK, PM-8-QAM, PM-16-QAM, PM-32-QAM and PM-64-QAM signals if the identifying features and decision thresholds are carefully chosen, even though the PM-M-QAM signals are insufficiently equalized by using the CMA. Note that 128-QAM and higher order modulation formats are not considered in the proposed MFI technique, since they are rarely utilized in practical systems due to their strict requirement to frequency and phase accuracy of the coherent optical receivers. Analytical models under additive Gaussian noise channel are built and successful MFI is realized within the range of OSNR starting from the theoretical minimum for 7%-overhead forward error correction (FEC) thresholds. Proof of concept experiments are also carried out for PM-QPSK, PM-16-QAM and PM-64-QAM signals generated from a pulse pattern generator (PPG), which confirms the feasibility of our proposed MFI technique in the dual-polarization long-distance fiber transmission systems.

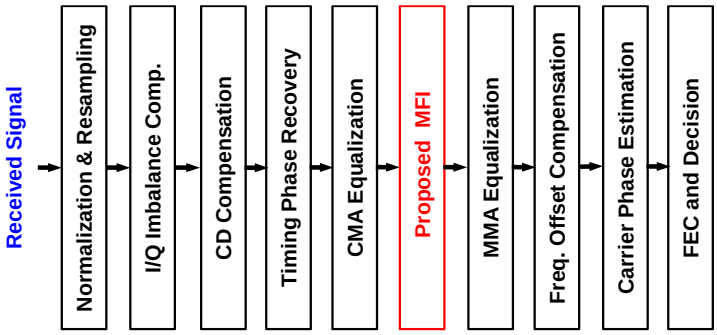

Fig. 1. Block diagram of digital signal processing algorithms in a digital coherent receiver supporting modulation format identification. CMA: constant modulus algorithm; MMA: multi- modulus algorithm.

2. Operating Principle

2.1 Identifying Feature Extraction

Fig. 2 shows the normalized power distributions of five common modulation formats including QPSK, 8-QAM, 16-QAM, 32-QAM and 64-QAM. Signals in presence of frequency offset and other phase impairments [shown in Fig. 2(b)] have the same normalized power distributions as that of the ideal constellations [Fig. 2(a)]. In a practical setting, the distribution can be obtained empirically from a block of received symbols if a sufficient symbol size is available. Clearly, different modulation formats have different power distributions, from which one can extract distinctive features for MFI. We propose to use ratios of probability of signal normalized power falling on different ranges as such decision metrics. Definitions of the three ratios R_1, R_2 and R_3 are shown in Table I. If proper decision rules are chosen, QPSK and 8-QAM signals can be identified from other signals by using ratio R_1, 64-QAM signals can then be distinguished by utilizing ratio R_2, and at last the 16-QAM signal can be separated from 32-QAM signals based on ratio R_3.

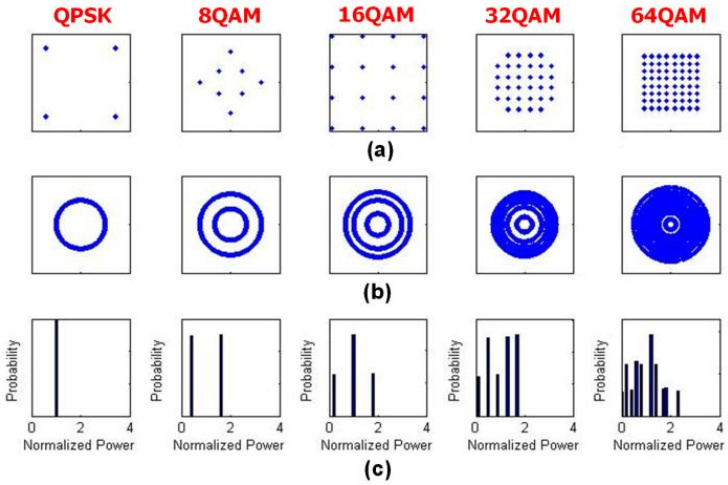

Fig. 2. (a) Ideal constellations; (b) signal constellations with large phase impairments; and (c) empirical probability distributions of normalized received signal powers for different modulation formats.

Table 1. Features of different modulation formats in the ideal situation

	Ratio R_1: $\frac{P_{(0.6 \le S \le 1.4)}}{P_{(S < 0.6 \cup S > 1.4)}}$	**Ratio R_2:** $\frac{P_{(2.1 \le S)}}{P_{(1.0 \le S < 1.1)}}$	**Ratio R_3:** $\frac{P_{(0.4 \le S \le 0.8)}}{P_{(S < 0.4 \cup 0.8 < S \le 1.2)}}$
QPSK	**∞**	**--**	**--**
8QAM	**0**	**--**	**--**
16QAM	**1**	**0**	**0**
32QAM	**0.6**	**0**	**1**
64QAM	**1**	**∞**	**--**

2.2 Modulation format identification under additive Gaussian noise channel

Bononi et al [20] showed that amplified spontaneous emission (ASE) noise as well as the fiber nonlinearity-induced noise can be approximated as additive Gaussian noise. As a result, the in-phase (I) and quadrature (Q) component of the received signal can be considered as independent Gaussian random variables with a variance of σ^2 and means μ_1 and μ_2, respectively. Then the probability density function (PDF) $f(x)$ of the normalized received power follows a non-central chi-squared distribution [21] given by

$$f(x) = \frac{1}{2\sigma^2} e^{-\frac{x+\nu^2}{2\sigma^2}} I_0\left(\frac{\nu\sqrt{x}}{\sigma^2}\right) \tag{1}$$

which has 2 degrees of freedom and $I_0(x)$ is the zero-order modified Bessel function of the first kind. The non-centrality parameter is

$$\frac{\nu^2}{\sigma^2} = \frac{\mu_1^2 + \mu_2^2}{\sigma^2} \tag{2}$$

For the received signals with normalized power, the OSNR is given by

$$OSNR = \frac{1}{2\sigma^2} \cdot \frac{B}{12.5e9} \tag{3}$$

where B is the symbol rate. Hence values of the ratios are dependent on optical signal-to-noise ratio (OSNR) of the received signals. Based on this model, the theoretical values of the three ratios R_1, R_2 and R_3 of 28 GBaud signals under additive Gaussian noise channel within OSNR range from 12 dB to 36 dB are shown in Fig. 3(a), (c) and (e), respectively. It can be seen that successful MFI is achieved by selecting proper decision thresholds [see orange dot line in Fig. 3(a), (c) and (e)] within the practical OSNR range for each modulation format.

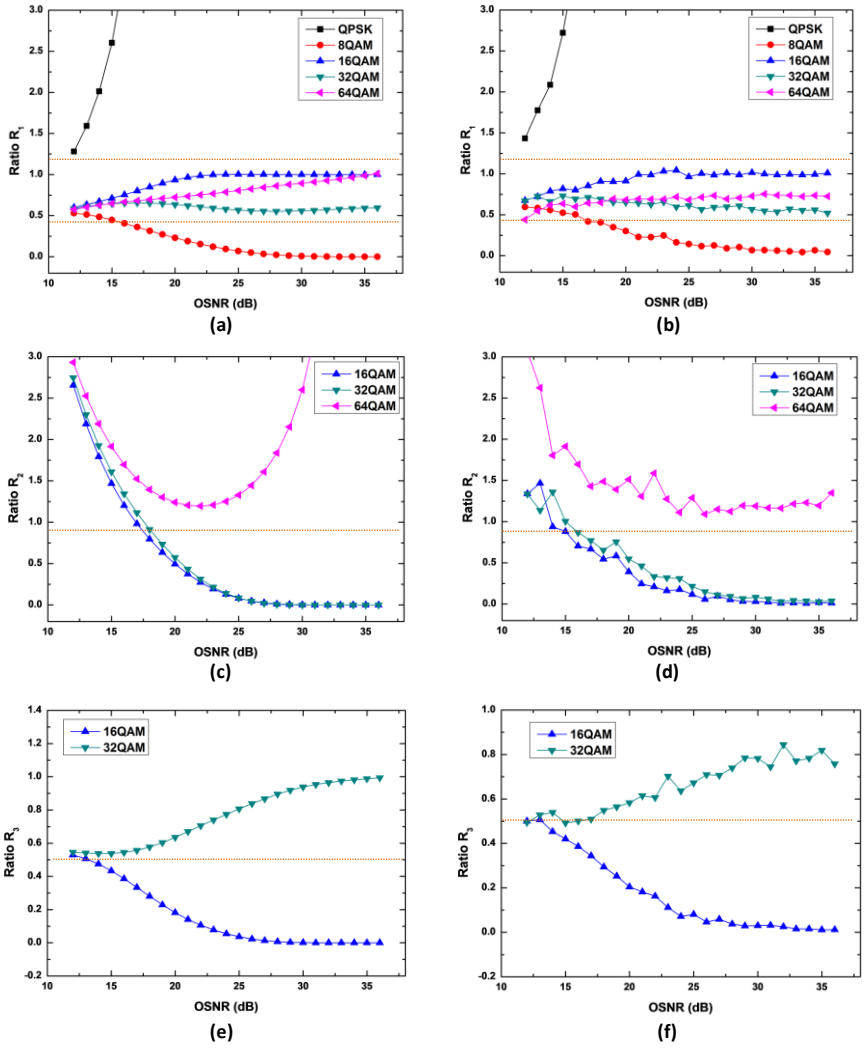

Fig. 3. The three ratios R_1, R_2 and R_3 under additive Gaussian noise channel (left column) and after CMA pre-convergence in dual-polarization systems (right column) as a function of OSNR from 12 to 36 dB. The orange dotted lines represent the decision thresholds.

2.3 Modulation format identification in dual-polarization systems

In the dual-polarization fiber-optic systems, in addition to the Gaussian noise, another issue that should be considered is polarization crosstalk. The commonly used multi-modulus algorithms (MMA) [19,22], which are often utilized following the CMA for M-QAM polarization demultiplexing, are dependent on the modulation format, and thus the MFI, locating before MMA in the DSP module (see Fig. 1), will be affected by the inefficient equalization of CMA. Although the recently proposed stokes space based polarization demultiplexing (SS-PDM) technique is modulation format independent [23], it could not equalize the residual CD not fully compensated by the static CD compensation algorithms and its performance will degrade when polarization-mode dispersion (PMD) exists [24], which will subsequently increase the complexity of MFI. Compared with SS-PDM, CMA performs more effective equalization to CD and PMD [25]. As a result, in this section, study is focused on the MFI after CMA equalization.

Since PM-M-QAM signals cannot be fully equalized and demultiplexed using solely standard CMA [19,26], the insufficient equalization after CMA will have an impact on the normalized power distribution of the M-QAM signals when they work in the dual-polarization systems. A proof-of-concept dual-polarization simulation setup with additive Gaussian white noise (AWGN) channel model was built to facilitate the analysis of signal normalized power distribution after CMA pre-convergence. In the simulation, the polarization rotation angle was set to $\pi/6$, while the PMD was around 4 ps. CMA with a step width of 1e-5 and a filter tap number of 21 was utilized in the simulation for equalization. Note that the value of step size of the CMA will affect both of the speed and accuracy of convergence. Considering the performance-versus-complexity trade-off, moderate values were set. The CMA with fixed parameters may degrade the performance of equalization, however, further equalization could be done by using the MMA with the knowledge of modulation format after the MFI block, as shown in Fig. 1. In addition, adaptive step-size CMA [27, 28] might be a good alternative to help improve the system performance, which is independent of the modulation format and can be used before the MFI block. Within OSNR range from 12 dB to 36 dB, the values of the three ratios R_1, R_2 and R_3 of the 28-Gbaud dual-polarization signals after CMA pre-convergence are shown in Fig. 3(b), (d) and (f), respectively. Compared with the results in Fig. 3(a), (c) and (e), the ratio values in dual-polarization systems have different trends as the OSNR increases. Especially for 64-QAM signal, the value of ratio R_2 in Fig. 3(d) is quite different from that in Fig. 3(c) even at an OSNR of more than 30dB. This deviation may be attributed to the insufficient equalization of the standard CMA algorithm. However, if we carefully choose a proper decision threshold for each ratio, considering the practical OSNR range for each modulation format, a good MFI performance can be ensured. The corresponding decision process for our proposed MFI is shown in Fig. 4.

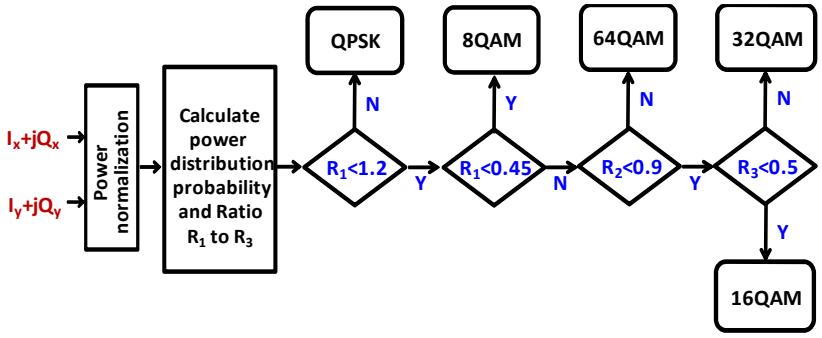

Fig. 4. Decision flow chart for the proposed MFI based on normalized signal power distributions

In order to verify the performance of the proposed MFI technique, 500 independent simulations of 28Gbaud QPSK, 8-QAM, 16-QAM, 32-QAM and 64-QAM transmissions in the dual-polarization system mentioned in previous paragraph were conducted for each OSNR value. 10000 symbols were utilized to form empirical distributions of received signal power for MFI in each run. A closer approximation to the theoretical distribution can be obtained by further increasing the number of symbols, at the cost of increasing the computational complexity. Using the decision flow chart described in Fig. 4, the probabilities of correct format identification at different OSNRs are shown in Fig. 5. It can be seen that virtually 100% correct identification is achieved for all the five modulation formats when their OSNRs exceed their respective FEC thresholds. Here OSNR thresholds corresponding to 7%-overhead FEC correcting bit error rate (BER) of 3.8e-3 was utilized, considering the tradeoff of the net coding gain and the complexity of the electronic components in practical system settings. In addition, it should be noted that the proposed MFI scheme mainly focus on identification of a single modulation format in each operation. When modulation formats of the received signals change, a new round of MFI should be performed. In practical implementations, the MFI functionality could be triggered at the time of network

reconfiguration, which might be realized by monitoring short loss of signal events at the receiver [17].

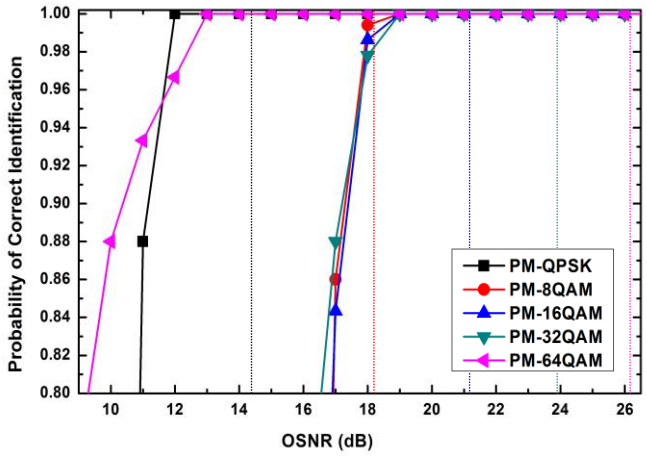

Fig. 5. Probability of correct identification vs. OSNR in the dual-polarization system. The dotted lines (same color with the corresponding data curves) denote FEC thresholds of the corresponding modulation formats. The specific values of the probabilities of correct identification at the FEC thresholds were also given in Table 1 for easy reading.

Table 1. Probabilities of correct format identification at their respective FEC thresholds of the five modulation formats

	28Gbaud PM-QPSK	**28Gbaud PM-8-QAM**	**28Gbaud PM-16-QAM**	**28Gbaud PM-32-QAM**	**28Gbaud PM-64-QAM**
FEC threshold at BER of 3.8e-3 (dB)	14.4	18.2	21.2	23.8	26.2
Probability of Correct Identification	100%	99.4%	100%	100%	100%

3. Proof-of-Concept Experiment

Experiments were conducted to investigate the proposed MFI technique among PM-QPSK, PM-16QAM and PM-64QAM systems. The experimental setup is shown in Fig. 6. At the transmitter side, an external cavity laser (ECL) at 1550.12nm was modulated with an I/Q modulator driven by multi-level electrical signals to generate 28Gbaud QPSK, 28Gbaud 16-QAM and 20Gbaud 64-QAM transmissions. The electrical signals utilized to generate 16-QAM and 64-QAM signals were generated from a pulse pattern generator (PPG) followed by two digital-to-analog converters (DACs) [29]. Here note that only 20G Baud rate was achieved for the 64-QAM signal generation because of the device limitation. Polarization multiplexing was realized through a polarization beam splitter (PBS), an optical delay line and a polarization beam combiner (PBC). The signals were amplified and launched into a fiber re-circulating loop consisting of a span of 80 km SSMF, an erbium-doped fiber amplifier (EDFA), an attenuator for OSNR adjustment and a 5-nm optical band-pass filter (BPF) for channel power equalization. After transmission through the loop, the received signal was filtered by a 3rd order Gaussian optical BPF with a 0.4-nm bandwidth followed by an integrated coherent receiver. The linewidth of the transmitter and the local oscillator (LO) were 150 KHz and 100 KHz, respectively. The frequency offset was set to

1 GHz. The coherently detected signal was sampled by a 50G sample/s real-time oscilloscope and then processed offline with the DSP described in the previous section, including normalization, re-sampling, CD compensation and CMA pre-equalization with step size of 1e-5 regardless of modulation format. In our experiments, 10000 symbols were used to generate the received power distribution for MFI.

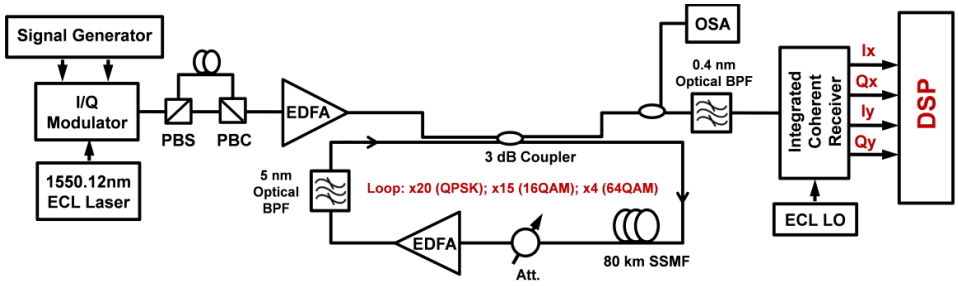

Fig. 6. Experimental setup for the proposed MFI technique. Att: attenuator, PC: polarization controller, BPF: band pass filter.

Fig. 7 shows the MFI performance for both back-to-back and 28 GBaud PM-QPSK, 28 GBaud PM-16-QAM and 20 GBaud PM-64-QAM transmissions over different fiber distance. As shown in Fig. 7(a), QPSK signals can be successfully distinguished from 16-QAM and 64-QAM signals when the threshold of ratio R_1 is set to 1.2 for virtually all OSNR values of interest. In addition, for OSNR exceeding 18 dB, Figure 7(b) shows that the 28GBaud PM-16-QAM signals can be clearly identified from the 20 GBaud PM-64-QAM signals by using ratio R_2 with threshold 0.9. Fig. 7(c) and (d) shows the ratios R_1 and R_2 respectively for different signal launched powers after fiber transmission. The results show that fiber nonlinearity does affect the received signal power distributions and hence the two ratios. Nonetheless, for realistic range of signal launched powers (see green marks in Fig. 7(c) and (d)), the same thresholds for R_1 and R_2 can properly identify the three signals, showing that the proposed MFI technique is resilient towards fiber nonlinear effects.

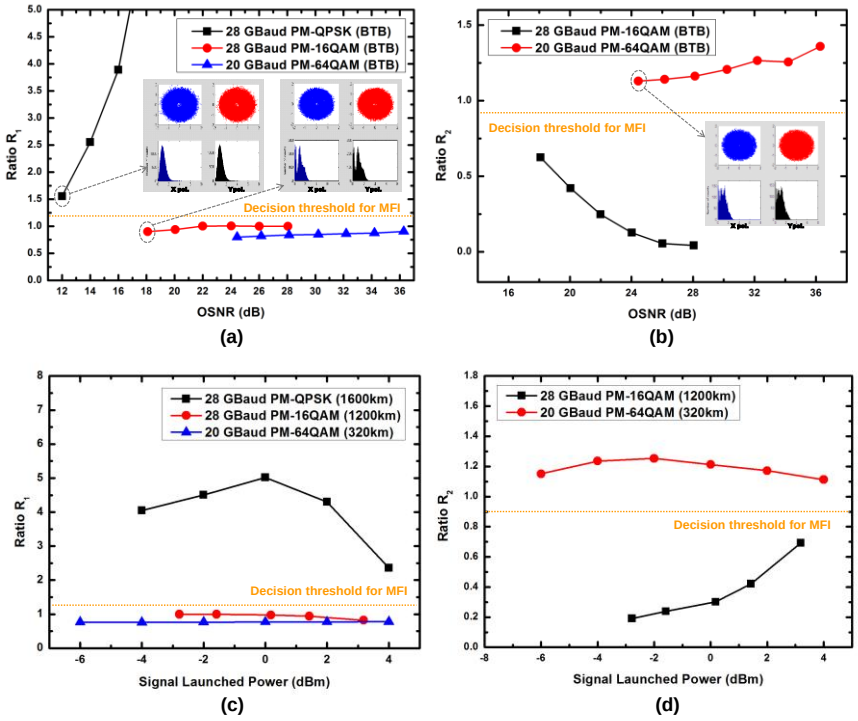

Fig. 7. (a) Ratio R1 and (b) Ratio R2 vs. OSNR for back-to-back transmissions.(inset: normalized received signal constellations and power distributions after CMA); (c) Ratio R1 vs. signal launched power for 1600 km (PM-QPSK), 1200 km(PM-16-QAM) and 320 km(PM-64-QAM) transmissions; (d) Ratio R2 vs. signal launched power for 1200 km(PM-16-QAM) and 320 km(PM-64-QAM) transmissions.

4. Conclusion

We have proposed a simple MFI technique based on distinctive features extracted from distributions of the normalized signal power for digital coherent optical receivers. The proposed method requires fairly simple DSP, needs no prior training and is insensitive to phase impairments. Moreover, it also performs good identification of PM-M-QAM signals even after insufficient CMA equalization. Successful MFI among QPSK, 8-QAM, 16-QAM, 32-QAM and 64-QAM signals was demonstrated in the dual polarization simulation systems. PM-QPSK, PM-16-QAM and PM-64-QAM signals were also successfully identified in the proof-of-concept experiment with practical OSNR and signal launched power ranges. Blind and real-time identification of modulation format make our MFI technique a good candidate for future digital coherent receivers of the CONs.

Acknowledgment

The authors would also like to acknowledge the generous support of the Hong Kong Polytechnic University [grant numbers G-YM17] and the Hong Kong Government General Research Fund [grant numbers PolyU 152079/14E]. This work was also supported in part by Natural Science Foundation of China under[grant numbers 61505266] and Natural Science Foundation of Guangdong Province, China [grant numbers 2014A030310364].

References

[1] E. Ip, A.P.T. Lau, D. Barros, and J. Kahn, “Coherent detection in optical fiber systems,” Opt. Express, 16(2), (2008)753-791.

[2] J. McDonough, “Moving standards to 100 Gbe and beyond,” IEEE Commun. Magazine, 45(11), (2007)6–9.
[3] S. J. Savory, “Digital coherent optical receivers: Algorithms and subsystems,” IEEE J. Sel. Top. Quantum Electron., 16(5), (2010)1164–1179.
[4] S. Yan, D. Wang, Y. Gao, C. Lu, A. P. T. Lau, Y. Zhu, Y. Dai and X. Xu, “Generation of 64-QAM Signals Using a Single Dual-Drive IQ Modulator Driven by 4-level and Binary Electrical Signals,” in Optical Fiber Communication Conference and Exposition and The National Fiber Optic Engineers Conference, Technical Digest (CD) (Optical Society of America, 2013), paper OM3C. 5.
[5] W. Wei, C. Wang, and J. Yu, “Cognitive optical networks: Key drivers, enabling techniques, and adaptive bandwidth services,” IEEE Communications Magazine, 50(2012) 106–113.
[6] K. Roberts, and C. Laperle, “Flexible Transceivers,” in European Conference and Exhibition on Optical Communication (ECOC) (2012), paper We.3.A.3.
[7] O. A. Dobre et al., “Survey of automatic modulation classification techniques: classical approaches and new trends,” IET Commun., 1(2), (2007)137-156.
[8] W. Wei and J. M. Mendel, “Maximum-likelihood classification for digital amplitude-phase modulations,” IEEE Trans. Commun., 48(2), (2000)189-193.
[9] K. C. Ho, W. Prokopiw, and Y. T. Chan, “Modulation identification of digital signals by the wavelet transform,” IEE Proc. Radar, Sonar and Navig., 147(4), (2000)169-176.
[10] G. Hatzichristos and M. P. Fargues, “A hierarchical approach to the classification of digital modulation types in multipath environments,” In Signals, Systems and Computers, Conference Record of the Thirty-Fifth Asilomar Conference on. IEEE , 2, (2001)1494-1498
[11] M. Selmi, Y. Jaouen and P. Ciblat "Accurate digital frequency offset estimator for coherent polmux QAM transmission systems," in European Conference and Exhibition on Optical Communication (ECOC) (2009), paper P3.08.
[12] I. Fatadin, D. Ives, and S. J. Savory, "Compensation of frequency offset for differentially encoded 16-and 64-QAM in the presence of laser phase noise," IEEE Photon. Technol. Lett., 22(3), (2010)176-178.
[13] N. Guerrero Gonzalez et al., “Cognitive digital receiver for burst mode phase modulated radio over fiber links,” in European Conference and Exhibition on Optical Communication (ECOC) (2010), paper P6.11.
[14] F. N. Khan et al., “Modulation format identification in heterogeneous fiber - optic networks using artificial neural networks,” Opt. Express, 20(11), (2012)2422-12431.
[15] R. Boada, R. Borkowski, and I. T. Monroy, “Clustering algorithms for Stokes space modulation format recognition,” Opt. express, 23(12), (2015)15521-15531.
[16] R. Borkowski, et al., "Stokes Space-Based Optical Modulation Format Recognition for Digital Coherent Receivers," IEEE Photonics Technology Letters, vol. 25, no. 21, pp. 2019-2032, Nov. 2013.
[17] P. Isautier, et al., "Stokes Space-Based Modulation Format Recognition Method for Autonomous Optical Receivers," IEEE Journal of Lightwave Technology, vol. 33, no. 24, pp. 5157-5163, Dec. 2015.
[18] J. Liu, Z. Dong, K. Zhong, A. P. T. Lau, C. Lu and Y. Lu, “Modulation Format Identification Based on Received Signal Power Distributions for Digital Coherent Receivers,” in Optical Fiber Communication Conference and Exposition and The National Fiber Optic Engineers Conference, Technical Digest (CD) (Optical Society of America, 2014), paper Th4D. 3.
[19] X. Zhou, “Digital signal processing for coherent multi-level modulation formats,” Chinese Optics Letters, 8(9), (2010) 863-869.
[20] A. Bononi, O. Beucher, and P. Serena. "Single-and cross-channel nonlinear interference in the Gaussian Noise model with rectangular spectra." Opt. Express, 21(26), (2013)32254-32268.
[21] M. K. Simon, Probability distributions involving Gaussian random variables: A handbook for engineers and scientists [M], Springer, 2007.
[22] X. Zhou, J. Yu, P. Magill, "Cascaded Two-Modulus Algorithm for Blind Polarization De-Multiplexing of 114-Gb/s PDM-8QAM Optical Signals," Optical Fiber Communication Conference, 2009.
[23] B. Szafraniec, B. Nebendahl, and T. Marshall, “Polarization demultiplexing in Stokes space,” OPTICS EXPRESS, 18(17), (2010) 17928-17939.
[24] B. Szafraniec, T. S. Marshall, and B. Nebendahl, “Performance monitoring and measurement techniques for coherent optical systems,” J. Lightw. Technol., 31(4), (2013) 648–663.
[25] I. Roudas, A. Vgenis, C. Petrou, D. Toumpakaris, J. Hurley, M. Sauer, J. Downie, Y. Mauro, and S. Raghavan, “Optimal polarization demultiplexing for coherent optical communications systems,” J. Lightw. Technol., 28(7), (2010)1121–1134
[26] D. Godard, “Self-recovering equalization and carrier tracking in two dimensional data communication systems,” IEEE Trans. Comm., 28(11), (1980)1867–1875,
[27] V. Zarzoso, and P. Comon, “Optimal step-size constant modulus algorithm,” IEEE Transactions on communications, 56(1), (2008)10-13.
[28] X. Di, C. Tong, X. Zhang, X-G. Zhang, and L. Xi, “Adaptive Step-Size Constant Modulus Algorithm for High-Speed Optical Coherent Communication System,” ACTA OPTICA SINICA, 32(10), (2012) 1006004-1-5.
[29] A. Gnauck, P. Winzer, S. Chandrasekhar, X. Liu, B. Zhu, and D.Peckham, “10 224-Gb/s WDM transmission of 28-Gbaud PDM 16-QAM on a 50-GHz grid over 1,200 km of fiber,” in *Proc. OFC 2010,* Paper PDPB8.